Title page

Title: Nonlinear biomarker interactions in conversion from Mild Cognitive Impairment to Alzheimer's disease

Running title: Biomarker interactions in Alzheimer's conversion

Authors:

Sebastian G. Popescu[1,5], Alex Whittington[1,2], Roger N. Gunn[2,3,4], Paul M. Matthews[4,5], Ben Glocker[5], David J Sharp[1] & James H Cole[1,7] for the Alzheimer's Disease Neuroimaging Initiative*

Affiliations:

[1]Computational, Cognitive & Clinical Neuroimaging Laboratory, Division of Brain Sciences, Imperial College London, London, UK.

[2]Invicro Ltd, London, UK.

[3]Department of Engineering Science, Institute of Biomedical Engineering, University of Oxford, UK.

[4]Division of Brain Sciences, Department of Medicine, Imperial College London, London, UK

[5]UK Dementia Research Institute.

[6]Biomedical Image Analysis Group, Department of Computing, Imperial College London, London, UK.

[7]Department of Neuroimaging, Institute of Psychiatry, Psychology & Neuroscience, King's College London, London, UK.

Corresponding author: James H Cole; Postal address: Centre for Neuroimaging Sciences, PO89, De Crespigny Park, Institute of Psychiatry, Psychology & Neuroscience, King's College London, London, SE5 8AF; email address: james.cole@kcl.ac.uk

*Data used in preparation of this article were obtained from the Alzheimer's Disease Neuroimaging Initiative (ADNI) database (adni.loni.usc.edu). As such, the investigators within the ADNI contributed to the design and implementation of ADNI and/or provided data but did not participate in analysis or writing of this report. A complete listing of ADNI investigators can be found at:

http://adni.loni.usc.edu/wpcontent/uploads/how_to_apply/ADNI_Acknowledgement_List.pdf

Abstract

Word count: 394/400

The multi-faceted nature of Alzheimer's disease means that multiple biomarkers (e.g., amyloid-β, tau, brain atrophy) may improve the tracking of disease progression and the prediction of health outcomes. However, the mechanisms relating these biomarkers to the disease are inter-related to a degree. Hence, optimally modelling the relationships between different Alzheimer's biomarker is warranted to reduce statistical uncertainty in predictions, to understand disease mechanisms, and to provide tools for clinical decision-making at the individual patient level.

Here, we used Gaussian Processes to model nonlinear interactions when combining biomarkers to predict Alzheimer's disease conversion in 48 mild cognitive impairment participants who progressed to Alzheimer's disease and 158 stable (over three years) people with mild cognitive impairment. Measures included: demographics, APOE4 genotype, CSF (amyloid-β42, total tau, phosphorylated tau), neuroimaging markers of amyloid-β deposition ([18^F]florbetapir) or neurodegeneration (hippocampal volume, brain-age). We examined: (i) the independent value each biomarker has in predicting conversion; and (ii) whether modelling nonlinear interactions between biomarkers improved prediction performance.

Despite the correlations between different biomarkers, our results show each measured added complementary information when predicting conversion to Alzheimer's disease. A linear model predicting MCI group (stable versus progressive) explained over half the variance in group (R^2 = 0.51, $P < 0.001$), with the top independently-contributing biomarker being hippocampal volume (R^2 = 0.13).

Next, we compared the sensitivity of different models to progressive MCI: independent biomarker models, additive models (with no interaction terms), nonlinear interaction models. We observed a significant improvement ($P < 0.001$) for various two-way interaction models, with the best performing model including an interaction between amyloid-β-PET and P-tau, while accounting for hippocampal volume (sensitivity = 0.77).

Our results showed that closely related biomarkers still contribute uniquely to the prediction of conversion, supporting the continued use of comprehensive biological assessments. However, our nonlinear interaction models suggest that for some patients, additional biomarkers may add little value (i.e., when hippocampal volume is high), but that for others (i.e., with low hippocampal volume) further invasive and expensive testing is warranted. Our results suggest that the interaction

between hippocampal atrophy and amyloid-deposition influences progression to Alzheimer's disease over and above their independent contributions, to a moderate extent. Our Gaussian Processes framework enables visual examination of these nonlinear interactions, allowing projection of individual patients into biomarker ‘space’, providing a way to make personalise healthcare decisions or stratify subsets of patients for recruitment into trials of neuroprotective interventions.

Keywords:

Alzheimer's disease; Mild Cognitive Impairment; biomarker interactions; Gaussian Processes

Abbreviations:

AUC = Area under the receiver operating characteristic curve

ADNI = Alzheimer's Disease Neuroimaging Initiative

Brain-PAD = Brain-predicted age difference

MCI = Mild Cognitive Impairment

P-tau = phosphorylated-tau

Standardized uptake value ratios = SUVR

Introduction

Rapid increases in the prevalence of Alzheimer's disease over the 21st century are predicted (Brookmeyer *et al.*, 2007), hence there is a pressing need to develop disease modifying treatments. Research diagnostic criteria have been proposed, reflecting key biological facets of Alzheimer's such as cerebral amyloid-β deposition, altered levels of proteins in CSF and neurodegeneration (Sperling *et al.*, 2011; Dubois *et al.*, 2014). It is hoped that these biological characteristics can be measured in people prior to symptoms manifesting, identifying at-risk individuals and enabling interventions to be targeted at slowing disease progression and delaying symptom onset.

Dynamic models of the transition to Alzheimer's have been proposed (Jack Jr *et al.*, 2010). These include a sequential model of biomarker relevance: CSF amyloid-β42, followed by cerebral amyloid-β deposition measured by PET, then CSF tau, followed by neurodegeneration measured by structural MRI. Cognitive impairment then develops prior to the onset of dementia (Jack Jr *et al.*, 2013). More recently, Jack and colleagues (2016) put forward a 'multi-state' transition model, with two distinct pathways; one where cerebral amyloid-β deposition occurs prior to neurodegeneration, and one where neurodegeneration occurs prior to amyloid-β deposition. This latter pathway also contained a potential transition from neurodegeneration to dementia without amyloid-β deposition. This adaptation is in line with the idea that amyloid-β deposition can be independent from imaging biomarkers of neurodegeneration (Draganski *et al.*, 2013).

This paradigm Alzheimer's progression of provides a valuable framework in which to test hypotheses about the underlying drivers of the disease. However, the specificity of this framework is limited, due to the highly heterogeneous Alzheimer's population (Tatsuoka *et al.*, 2013). For example, although the accumulation of amyloid-β plaques is a defining pathological feature of Alzheimer's, many cognitively-normal older adults also have elevated amyloid-β plaque levels (Villemagne *et al.*, 2011). Thus amyloid-β deposition is not solely sufficient to cause dementia (Aizenstein *et al.*, 2008). Furthermore, while CSF tau was found to positively correlate with severity of cognitive impairment (Shaw *et al.*, 2009), increased CSF tau appears to indicate neuronal injury and neurodegeneration in different diseases (Schoonenboom *et al.*, 2011). Neurodegeneration, or brain atrophy, though commonly seen in Alzheimer's, is also observed in many neurological diseases (Lorenzetti *et al.*, 2009; Chaudhuri, 2013) and in normal ageing (Fjell *et al.*, 2009). Even hippocampal atrophy, often cast as a key characteristic of Alzheimer's, can be seen in many other neurological and psychiatric conditions (Laakso *et al.*, 1996; reviewed by Cole, 2018). More work is needed to incorporate the heterogeneity of Alzheimer's into disease biomarker models. This should

improve specificity and better enable treatment decisions to be made at the individual level, to aid in clinical practice and evaluate potential treatments.

To improve specificity in the use of biomarkers for staging Alzheimer's, multiple measures are likely to be necessary. This way, complementary information from different biological sources can be combined to build a more comprehensive picture of the underlying diseases processes, and hopefully capture disease heterogeneity more accurately. An essential consideration when combining these multiple sources of information is how they interact. For instance, while amyloid-β deposition may precede and potentially drive subsequent neurodegeneration in some instances, the magnitude of amyloid-β deposition is likely to be key. An individual may be 'positive' for amyloid-β on a PET scan but remain below some latent threshold for neuronal or glial loss. Once over that threshold, neurodegeneration might occur. Equally, some individuals may have been exposed to negative genetic or environmental factors, not necessarily Alzheimer's related, that have influenced the rate of age-associated change in brain structure contributing to cognitive impairment. On this back-drop of poorer brain health, potentially only minimal amyloid deposition is necessary to cause cognitive impairment.

While much research using machine learning to predict conversion from MCI to Alzheimer's has been conducted (Sarica *et al.*, 2017; Pellegrini *et al.*, 2018), only a limited number of studies have specifically looked into modelling biomarker interactions. Importantly, prior studies also have only considered linear interactions. For example, Li and colleagues (2014) implemented a weak-hierarchical interactions model to impose sparsity in modelling pairwise interactions between biomarkers derived from T1-weighted scans and cognitive scores. Caroli and colleagues (2015) found greater disease progression rates in subjects 'positive' for both CSF amyloid-β42 and hippocampal volume compared to those with just one of the aforementioned risk profiles. Secondly, Pascoal and colleagues (2017a) suggested that the interactions between voxel-level amyloid-β-PET SUVR and CSF phosphorylated-tau (p-tau) levels were important for predicting two-year metabolic decline in basal and mesial temporal, orbitofrontal, and anterior and posterior cingulate cortices. In related work, Pascoal and colleagues (2017b) reported that being positive for both amyloid-β-PET and CSF p-tau is the strongest factor associated with developing dementia. Bilgel and colleagues (2018) conducted linear mixed-effects analyses to assess cross-sectional and longitudinal trends in cognitive test scores by amyloid-positive and neurodegeneration-positive groups, detecting synergistic effects between hippocampal volume and amyloid-β-PET. Lastly, Fotea and colleagues (2014) used vertex-wise linear interaction model to assess whether cortical thinning is caused by a synergy between amyloid-β-PET and p-tau.

Linear models may be limited intrinsically, as many of the relevant biological interactions are non-linear, and may be described by models that incorporate thresholds, plateaus and other complex relationships. One approach to modelling non-linear interactions is to use Gaussian Processes, a family of models that assigns to each biomarker a nonparametric smoothing function, allowing effects of non-linearities in both additive (i.e., main effects) and interaction models to be captured. Here, we tested the hypothesis that the conversion from MCI to Alzheimer's can be better predicted by modelling biomarkers interactions (linear or non-linear), than by using the additive sum of independent effects on disease progression. For example, patients with low CSF amyloid-β42 may be more likely to convert if this is combined with neurodegeneration, either at local or global level, than if they are not subject to neurodegeneration and the CSF amyloid-β42 reductions are occurring in isolation. Using the commonly-studied ADNI dataset, we analysed people with stable and progressive MCI to investigate: (i) the independent value each biomarker has in predicting conversion; and (ii) whether modelling two-way and higher-order non-linear interactions between biomarkers could improve the log likelihood value of predictions of conversion to Alzheimer's on unseen data.

Here, we included multiple biological indices, to capture different facets of Alzheimer's: APOE genotype, CSF measures of amyloid-β42, total tau and p-tau, PET measure of amyloid-β deposition, and structural MRI measures of global 'brain age' and specific hippocampal volume. Our motivation to use brain-age was based on previous work that showed that having an older-appearing brain is associated with conversion to Alzheimer's within three years, and is more statistically informative than hippocampal volume (Franke *et al.*, 2010; Franke and Gaser, 2012; Gaser *et al.*, 2013). Specifically, we used our previously-developed machine learning approach to generate a 'brain-predicted age' value from patterns of volumetric data contained in T1-weighted MRI scans (Cole *et al.*, 2017b). This technique defines a regression model of healthy brain ageing based on scans from a large independent healthy sample, which allows accurate prediction of age in new individuals. We have used this technique to demonstrate abnormal brain-ageing after a traumatic brain injury, in treatment resistant epilepsy and Down's syndrome (Cole *et al.*, 2015; Cole *et al.*, 2017a; Pardoe *et al.*, 2017). Brain-predicted age also relates to cognitive performance and mortality risk in older adults from the general population (Cole *et al.*, 2018), suggesting that this metric reflects something of the brain's sensitivity to more general health, and thus could be relevant for assessment of resilience to disease progression in neurodegenerative contexts.

Material and methods

Participants

Participants were drawn from the publicly-available ADNI dataset. Inclusion criteria included the availability of all biomarkers (genetic, fluid, PET, MRI), a diagnosis of MCI at baseline imaging assessment and the availability of clinical follow-up three years after the imaging assessment to determine disease progression. Stable MCI participants still met the criteria for MCI after three years; progressive MCI participants met the criteria for a clinical diagnosis of dementia at or before the three-year assessment. In total, n = 206 people with MCI were included in the analysis; stable MCI n = 158 (age range 55-89 years, median age=71.60 years), progressive MCI n = 48 (age range 55-84 years, median age = 73.85 years). Further participant details are included in Table 1.

ADNI is a longitudinal observational study investigating whether serial brain imaging, clinical, and neuropsychological assessments can be combined to measure the progression of AD. Detailed information regarding the ADNI study's procedures, including participant inclusion and exclusion criteria, and the complete study protocol can be found at http://adni.loni.usc.edu/. ADNI was launched in 2003 as a public-private partnership, led by Principal Investigator Michael W. Weiner, MD. ADNI is the result of efforts of co-investigators from a broad range of academic institutions and private corporations with participants being recruited from over 50 sites across the U.S and Canada. To date, there are over 1500 adults, aged between 55 and 90, that participated in its three studies (ADNI-1, ADNI-GO, ADNI-2). The primary goal of ADNI has been to test whether serial MRI, PET and other biological markers, and clinical and neuropsychological assessment could be combined to measure the progression of MCI and early Alzheimer's disease.

Table 1. Participant characteristics and biomarker values

Characteristic/biomarker	**Stable MCI**	**Progressive MCI**	**P-value (group comparison)**
n	158	48	-
Age, mean (SD), years	71.32 (7.24)	73.35 (6.76)	0.076
Gender n (%), female/male	41.77 (66/92)	45.83 (22/26)	-
APOE genotype n (%), ε4 carrier/no ε4 allele	39.24 (62/96)	70.83 (34/14)	-
Amyloid-β42, mean (SD)	190.8 (199.5)	139.32 ±35.36	<0.001
Total tau, mean (SD)	74.83 (41.73)	118.12 (55.84)	<0.001
Phosphorylated tau, mean (SD)	33.15 (18.58)	54.15 (27.94)	<0.001

Amyloid-β-PET SUVR, mean (SD)	1.34 (0.23)	1.56 (0.23)	<0.001
Hippocampal volume, bilateral mean (SD), mm^3	7268 (1056.87)	6219.23 (1016.33)	<0.001
Brain-PAD, mean (SD), years	-2.94 (7.93)	2.26 (8.37)	<0.001

Paired T-test were carried out to assess group differences. P values were uncorrected for multiple comparisons.

APOE4 = apolipoprotein e4; Brain-PAD = brain predicted age difference.

Biomarker analysis

A high-level overview of the methods used in the study is included in Figure 1.

Biomarkers: Genetics

APOE genotype was determined from a 10ml blood sample taken during study screening and sent overnight to the University of Pennsylvania ADNI Biomarker Core laboratory for analysis. The APOE genotype of each participant was recorded as a pair of numbers indicating which two alleles were present; either ε2, ε3 or ε4.

Biomarkers: Fluid

Samples of 20ml of CSF were obtained from participants by a lumbar puncture with a 20- or 24-gauge spinal needle, around the time of their baseline scan. All samples were sent same-day on dry ice to the University of Pennsylvania ADNI Biomarker Core laboratory. There, levels of the proteins (amyloid-β42, total tau, and p-tau) were measured and recorded, as described previously(Shaw *et al.*, 2009). By design, only a subset of ADNI participants had measurement of CSF levels.

Biomarkers: PET

Cerebral amyloid-β deposition was indexed using the PET tracer [18^F]florbetapir (F-AV45). PET imaging was performed within two weeks of the baseline clinical assessments, as described previously (Jagust *et al.*, 2015). In brief, four late-time five-minute frames are co-registered and averaged. The resulting image is converted to a 160x160x96 voxel static image with voxel dimension of $1.5mm^3$. Finally, an 8mm full-width half-maximum Gaussian kernel was applied (corresponding to the lowest resolution scanner used in the study). These primary data were downloaded from the ADNI database and used in the subsequent analyses.

F-AV45 data were nonlinearly registered into Montreal Neurological Institute 152 space (MNI152 space) using DARTEL (Ashburner, 2007). Initially the structural MRI images were segmented into grey matter and white matter using the Statistical Parametric Mapping (SPM12) software package

(University College London, UK) and registered to a group average template. The group average template was then registered to MNI152 space. The F-AV45 standardized uptake value ratio (SUVr) image for each participant was registered to the corresponding T1-weighted MRI using a rigid-body registration. Finally, the individuals' DARTEL flow field and template transformation was applied without modulation resulting in F-AV45 images in MNI152 space. The normalised maps were spatially smoothed (8mm full-width half-maximum Gaussian kernel). A neuroanatomical atlas (Tziortzi *et al.*, 2011) and a grey-matter probability atlas in MNI152 space were employed to calculate regional SUVr values. SUVr values were quantified using the grey matter cerebellum as the reference region (defined as the intersection between the cerebellum region from the anatomical atlas and the grey-matter atlas, thresholded at $p>0.5$). The mean uptake value for cerebellar grey matter was obtained and each image was divided by this to generate an SUVr image for each participant. Finally, an average cortical SUVr value was obtained by calculating the mean SUVr value for all cortical regions (weighted by regional volume).

Biomarkers: Structural MRI

Three-dimensional T1-weighted MRI scans were acquired at either 1.5T (ADNI-1) or 3T (ADNI-2 and ADNI-GO) suing previously described standardized protocols at each site (Jack et al., 2008). All MRI scans were pre-processed using SPM12. This entailed tissue segmentation into grey matter and white matter, followed by a nonlinear registration procedure using DARTEL (Ashburner, 2007) to MNI152 space, subsequently followed by resampling to $1.5mm^3$ with a 4mm Gaussian smoothing kernel.

Processed grey matter and white matter images were then entered in the Pattern Recognition for Neuroimaging Toolbox (PRoNTo) software (Schrouff *et al.*, 2013). Using a previously trained model that predicts chronological age from structural neuroimaging data, as per our previous work (Cole *et al.*, 2015; Cole *et al.*, 2017a; Cole *et al.*, 2017c; Cole *et al.*, 2018), we generated a brain-predicted age value for each participant. This step used a Gaussian Processes regression model with a linear kernel, with processed neuroimaging data as the independent variables, and age as the dependent variable. The training dataset used to define the model included n=2001 health adults aged 18-90 years; further details have been reported previously (Cole *et al.*, 2017b). Finally, we generated brain-PAD values; chronological age subtracted from brain-predicted age (i.e., the model predictions).

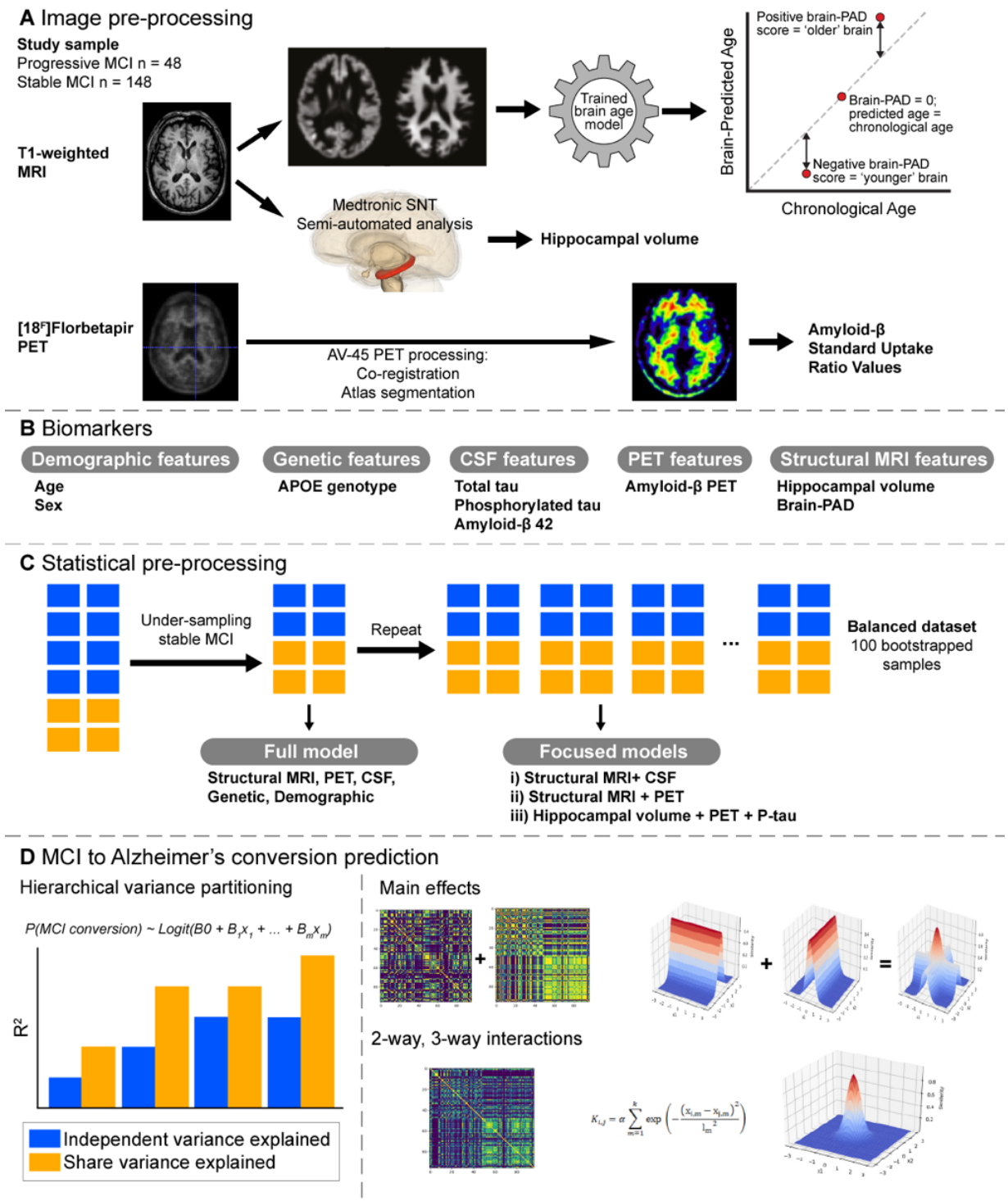

Figure 1. Overview of study methods

A) Raw T1-weighted MRI scans are pre-processed via the DARTEL pipeline in SPM12 to obtain grey matter and white matter volume maps. These are fed into a pretrained Gaussian Processes Regression based "brain-age" prediction software to arrive at an estimation of Brain-PAD, which is the difference between chronological age and neuroimaging-predicted "brain-age". B) CSF features and hippocampal volume alongside genetic and demographic information are also used as biomarkers; C) Subsampling stable MCI to alleviate the class imbalance issue. Repeat random subsampling of stable MCI 100 times for Gaussian

Processes based models; D) Partitioning of total variance explained into independent and shared variance explained for each biomarker; Gaussian Processes that allow just for main effects of biomarkers to be modelled are constructed by adding all the univariate squared exponential kernels corresponding to each biomarker. Full-order interactions between all biomarkers considered are captured through a single multivariate squared exponential kernel; Full set of statistics (sensitivity, specificity, accuracy, AUC) are computed for each replicate. Paired t-tests are conducted between accuracy scores stemming from main effects models and a model containing a multivariate kernel to assess if the increase in generalisation to unseen data is statistically significant.

Statistical analysis

Hierarchical partitioning of variance

We examined the independent contribution of each biomarker for distinguishing between stable and progressive MCI participants in a multivariate model, using hierarchical partitioning of variance (Chevan and Sutherland, 1991). Here, a hierarchical series of logistic regression models are fit, with all possible combinations of biomarkers. By comparing the variance explained by each model across all other models, an unbiased approximation of the variance attributable to each variable can be derived, both that independent of all other variables and that shared with other variables (due to the correlations between them).

Hierarchical partitioning of variance was carried out using the R package 'hier.part' with the following variables: age, sex; genetics (APOE4 genotype); CSF (amyloid-β42-CSF, total tau, p-tau); PET (amyloid-β-PET); structural MRI (hippocampal volume, brain-PAD). The number of variables was limited to nine as per Olea and colleagues (2010) to avoid inconsistent results. Thus, robust estimates of independent variance explained are obtained for each biomarker, which enabled assessment of the utility of including each biomarker when adjusting for all other biomarkers.

Multivariate biomarker models

We considered multiple statistical models, all with group (i.e., stable or progressive MCI) as the outcome (i.e., dependent) variable and with age, sex and APOE genotype as covariates. Each of the six imaging or fluid biomarkers were evaluated separately, alongside three different multivariate models, and a full model containing all biomarkers:

i. Hippocampal volume + brain-PAD + amyloid-β42-CSF
ii. Hippocampal volume + brain-PAD + amyloid-β-PET
iii. Hippocampal volume + amyloid-β-PET + p-tau
iv. Full model (hippocampal volume + brain-PAD + amyloid-β42-CSF + p-tau + total tau + amyloid-β-PET)

Gaussian Processes classification

Gaussian Processes are a supervised learning algorithm, that has found applications in many fields including our previous neuroimaging research (Cole *et al.*, 2015), due to its Bayesian and non-parametric properties. The principal behind Gaussian Processes is that a measured (dependent) variable is modelled by defining a multivariate Gaussian distribution, hence we can view them as being a distribution over functions (Rasmussen and Williams, 2006).

To obtain Gaussian Process models where our predictor variables are independent, we assigned to each biomarker an individual squared exponential kernel, and subsequently all kernels are added together to derive a global kernel. To introduce interactions between biomarkers, we used all the covariates within the same squared exponential kernel. Duvenaud and colleagues (2011) proposed that this kernel construction defines an *m*-order interaction over covariate space, where *m* is the total number of covariates used in building the kernel. For example, two-way interactions were constructed by assigning the respective two biomarkers to a single kernel, subsequently adding this to the list of univariate kernels specific to each biomarker. For all models we used the non-sparse version of the Scalable Variational Gaussian Processes Classifier (Hensman *et al.*, 2015).

Bootstrapping to adjust for class imbalance

The two groups of MCI patients were of differing size (progressive MCI n = 48, stable MCI n = 158), resulting in a class imbalance. To counter this imbalance, we subsampled the majority class (i.e., stable MCI) to generate a balanced dataset. To reduce the impact of sampling bias on this approach, we used bootstrapping (100 iterations) to randomly subsample the stable MCI group to create 100 different subsets, each compared with the entire progressive MCI group. Importantly, within each bootstrap, we used 10-fold stratified cross-validation to generate classification predictions for each participant. Sensitivity, specificity, (balanced) accuracy, area under the curve (AUC) and log likelihood values were calculated for each bootstrapped dataset. Values were then averaged across the 100 bootstrapped iterations.

Model comparisons

Two-way or three-way interactions were assessed by their relative improvement in log likelihood values compared to their corresponding main effects model. A paired t-test is used to test for differences, with the significance level set at 0.05. A list of the two-way and three-way interactions tested can be found in Table 2. To determine whether Gaussian Processes for classification resulted in improvements over less complex linear models, we performed the same classification task using logistic regression, with the same combination of different input variables and interaction terms

(Supplementary Table S2). When considering model performance, we opted to focus on sensitivity to detecting progressive MCI as the chief criteria, under the assumption that a false-negative classification of stable MCI, is clinically more deleterious than a false positive.

Data availability

All data used for the preparation of this article was obtained from ADNI and are publicly-available. For up-to-date information, see www.adni-info.org. Our statistical analysis code is available online (https://github.com/SebastianPopescu/nonlinear_interaction_GPs).

Results

A total of n = 158 stable MCI participants and n = 48 progressive MCI participants were included in our study. The two different groups are well matched in age and gender. In terms of APOE4 status, there is a significant difference, with 70.83% of progressive MCI being APOE4 positive, in comparison with 39.24% for stable MCI. Group differences were observed for all other biomarkers (Table 1).

Biomarkers capture independent facets of Alzheimer's progression risk

Hierarchical partitioning of variance was used to determine unique contributions of different predictor variables as well as their shared contribution towards prediction of conversion from MCI to Alzheimer's after three years. The total variance explained by this additive model was $R^2 = 0.51$, $P < 0.001$. Independent R^2 values were: age = 0.028, sex = 0.004, APOE4 = 0.069, amyloid-β42-CSF = 0.063, total tau = 0.054, p-tau = 0.045, amyloid-β-PET = 0.048, hippocampal volume = 0.126, brain-PAD = 0.076. A substantial proportion of the variance was shared between variables, indicating that these biomarkers reflect some common as well as unique processes underlying progression from MCI to Alzheimer's (Figure 2).

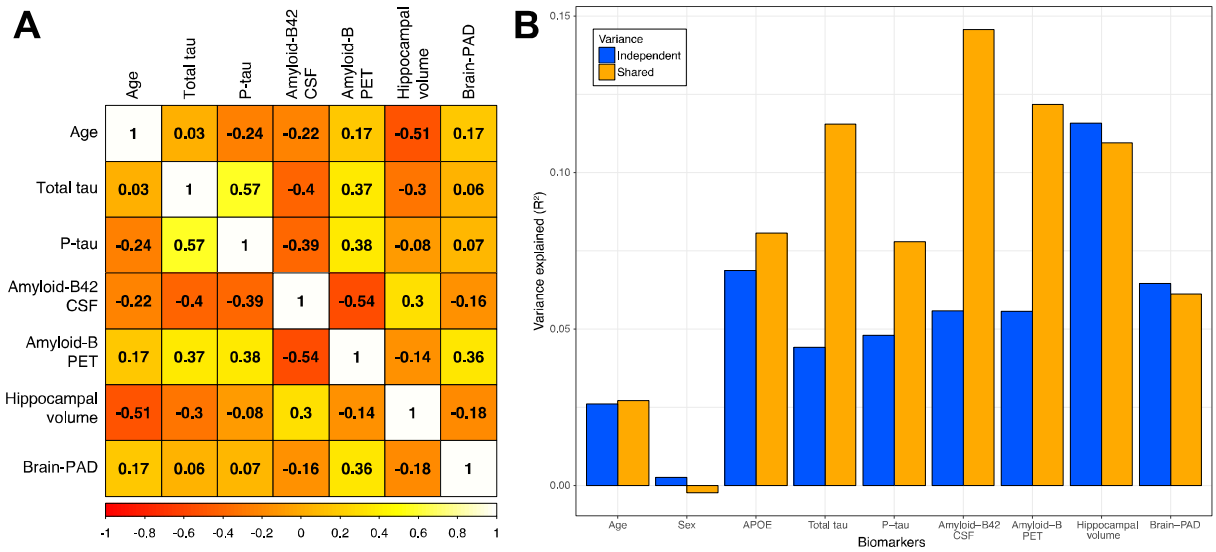

Figure 2. Independent and shared variance across biomarkers in predicting conversion to Alzheimer's

A) Correlation matrix of numerical biomarkers, showing Pearson's r values in balanced sub-sample of stable and progressive MCI participants (n = 96). B) Estimates of independent and shared variance for individual biomarkers in a logistic regression model with conversion to Alzheimer's labels as the outcome variable and age, sex, APOE genotype, total tau, P-tau, amyloid-β42-CSF, amyloid-β-PET, hippocampal volume and brain-PAD as predictors. Estimates derived from hierarchical partitioning of the variance, with blue bars indicating independent (i.e., unique) variance attributable to each biomarker and yellow indicating variance shared with one or more other biomarkers.

Nonlinear interactions between hippocampus and amyloid-based biomarkers

Different models were compared to assess the influence of including nonlinear interactions when classifying stable from progressive MCI (Table 2). For the models using biomarkers separately, P-tau showed the best sensitivity (0.729), while amyloid-β42-CSF had the top balanced accuracy (0.760). However, the AUC values for all these independent measures was broadly equivocal (AUCs range 0.722-0.749), except for brain-PAD, which was lower (AUC=0.637). For the additive models of main effects, sensitivity ranged from 0.712-0.770. When adding interaction terms for Model 1, we found that a bivariate interaction between hippocampal volume and amyloid-β42-CSF significantly improves model fit (i.e., significantly lowers log-likelihood). For Model 2, a two-way interaction between hippocampal volume and amyloid-β-PET also improved model fit. For Model 3, all three interactions improved model fit. That is, amyloid-β-PET by P-tau; amyloid-β-PET by hippocampal volume; P-tau by hippocampal volume. Finally, the inclusion of a three-way interaction between hippocampal volume, amyloid-β-PET and CSF P-tau also improved model fit for Model 2 and Model 3, but not Model 1. Notably, the sensitivity (range 0.708-771) and specificity (range 0.749-0.848) of the interaction models was similar to those of the additive main-effect models.

Logistic regression does not benefit from interaction terms

When using logistic regression to classify stable and progressive MCI patients, performance was moderately accurate, with balanced accuracies ranging from 0.67-0.72 (see Supplementary Table S2). Notably, for all models, classification sensitivity (range 0.61-0.65) was substantially lower than specificity (range 0.86-0.88), indicating that the logistic regression was better at identifying stable MCI patients than progressive MCI patients. When comparing the models containing interactions terms with their additive counterparts, t-tests showed than none of the interaction models were significant. This indicates that using standard logistic regression methods, where interactions are linear, there is no improvement in classification performance when including interaction terms.

Visualising nonlinear interactions

The most improvement performance came when including a two-way nonlinear interaction between amyloid-β-PET and hippocampal volume when adjusting for P-tau (Model 3). To interrogate the relationships between these three biomarkers by comparing the decision boundaries between the main effects model and including interaction terms (Figure 3). It is evident that for different levels of P-tau (based on this illustrative tertiary split), the relationship between hippocampal volume and amyloid-β-PET changes. In particular, for participants with medium P-tau levels, the predictive decision boundary better models the distribution of stable and progressive MCI participants.

Table 2. Biomarker model performance for predicting conversion from MCI to Alzheimer's

Model	Predictors	Sensitivity	Specificity	Balanced accuracy	AUC	T-test log likelihood, P-value
	Individual biomarkers					
	Amyloid-β42-CSF	0.625	0.895	0.760	0.749	-51.10
	Total tau	0.708	0.625	0.671	0.730	-58.88
	P-tau	0.729	0.666	0.697	0.722	-58.57
	Amyloid-β-PET	0.666	0.666	0.666	0.729	-58.09
	Hippocampal volume	0.666	0.666	0.666	0.739	-57.84
	Brain-PAD	0.645	0.604	0.625	0.637	-63.361
	Main effects					
1	Hippocampal volume, brain-PAD, amyloid-β42	0.712	0.842	0.777	0.866	-39.47
2	Hippocampal volume, brain-PAD, amyloid-β-PET	0.756	0.754	0.755	0.830	-45.44
3	Hippocampal volume, amyloid-β-PET, P-tau	0.770	0.762	0.766	0.830	-45.44
	Full model	0.770	0.729	0.760	0.838	-46.58
	Two-way interactions					
1	Brain-PAD * amyloid-β42	0.708	0.848	0.778	0.864	-39.45, 0.797
	Amyloid-β42 * hippocampal volume	0.713	0.846	0.780	0.865	-39.08, <0.001
2	Brain-PAD * amyloid-β-PET	0.759	0.749	0.754	0.826	-45.39, 0.46
	Hippocampal volume * amyloid-β-PET	0.723	0.788	0.756	0.830	-44.60, <0.001
3	Amyloid-β-PET * P-tau	0.771	0.756	0.764	0.826	-45.26, 0.015
	Hippocampal volume * amyloid-β-PET	0.733	0.806	0.769	0.840	-43.02, <0.001
	P-tau * hippocampal volume	0.758	0.768	0.763	0.826	-45.114, 0.003
	Three-way interactions					
1	Hippocampal volume * brain-PAD * amyloid-β42	0.724	0.830	0.777	0.861	-39.422, 0.745
2	Hippocampal volume * brain-PAD * amyloid-β-PET	0.738	0.791	0.764	0.827	-44.712, <0.001
3	Hippocampal volume * amyloid-β-PET * P-tau	0.748	0.812	0.780	0.835	-43.232, <0.001

AUC = Area Under Receiver Operator Characteristic Curve. T-tests (paired) based on comparison between accuracy and log likelihood scores on 100 bootstrapped sets are provided as a mean to assess the relative increase in generalisation attributable to the introduction of either two-way interactions or three-way interactions between biomarkers in comparison to main effects only variants.

Figure 3. Decision boundaries for the hippocampal volume, amyloid-β-PET and P-tau classification model.

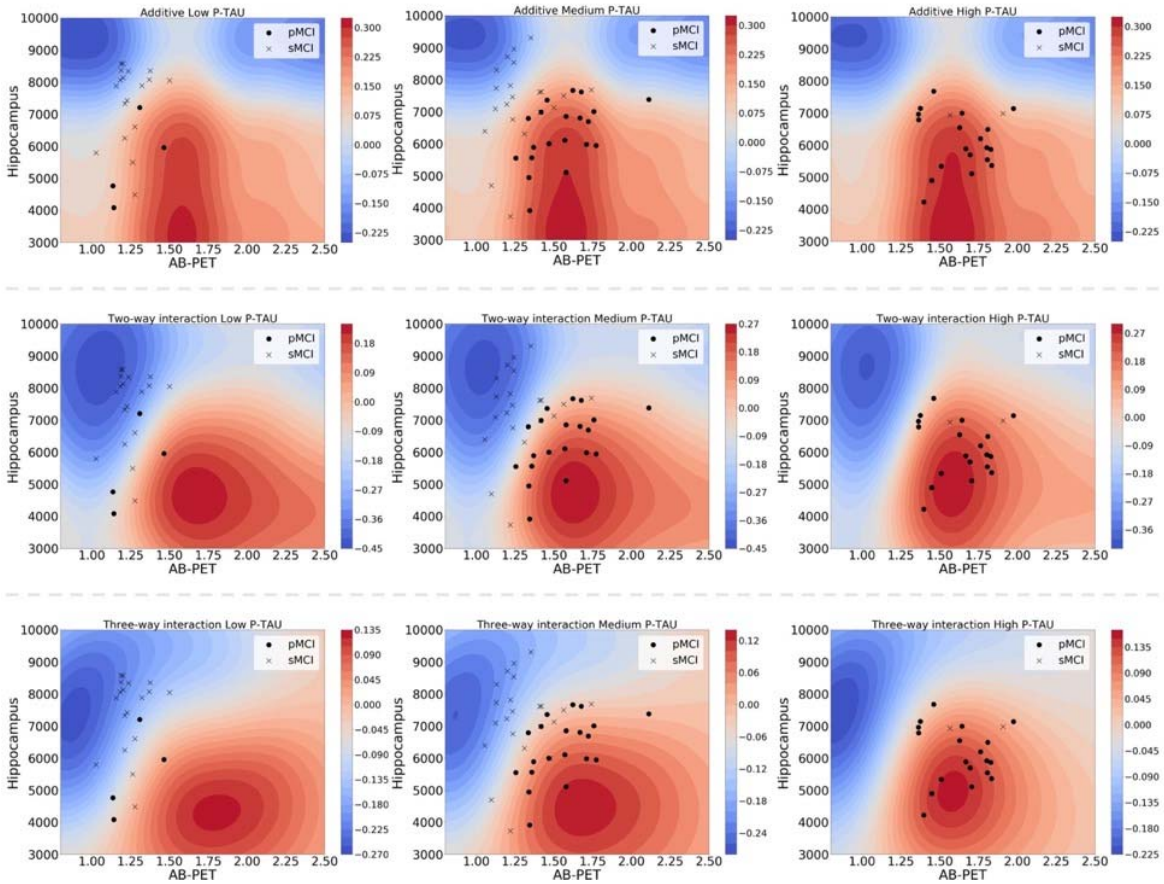

Data based on Model 3. Contour plots illustrate the decision boundaries for different classification models. Positive values (red contours) indicate regions where the probability of being classified as progressive MCI is increased; negative values (blue contours) where that probability is decreased. Scatterplots of amyloid-β-PET (x-axis) and hippocampal volume (y-axis) are overlaid (crosses = stable MCI, dots = progressive MCI), with each column representing a tertiary split of participants based on P-tau values (<22.22 = low P-tau, 22.22-36.25 = medium P-tau; >36.25 = high P-tau). A) Additive model (no interactions). First row captures the dynamics of the summation of the univariate kernels associated to each biomarker, as P-tau is increased from. B) Two-way interaction model. Values on this row represent how much information towards prediction the interaction term is adding on top of the univariate kernels. C) Three-way interactive model. The relative contribution of the three-way interaction between the biomarkers.

Discussion

Here, we modelled nonlinear interactions between a panel of biomarkers (neuroimaging, genetic, CSF) to predict disease progression from MCI to Alzheimer's disease. Statistical models that included nonlinear interaction term explained conversion risk moderately better than additive linear models, though the influence of these interaction models of the sensitivity to progressive MCI was negligible. Importantly, our panel of biomarkers all independently explained a proportion of the variance in a logistic classification model. Though unsurprising, given the existing literature

outlining the influence of these biomarkers in Alzheimer's (Jack *et al.*, 1999; Gaser *et al.*, 2013; Xu *et al.*, 2013; Caminiti *et al.*, 2018), this justifies the inclusion of different sources of information, despite the evident shared variance (i.e., bivariate correlations) between biomarkers. This is even the case for measures of amyloid; whereby the PET-derived and CSF-derived measures were correlated r = -0.54. Evidently some of the non-shared variance between these two biomarkers still relates to disease progression. This is in line with previous findings (Mattsson *et al.*, 2014), which showed that amyloid-β42-CSF and amyloid-β-PET provide partially independent information about a wide range of Alzheimer's measures. While a practitioner's decision about whether to acquire PET or CSF measures of amyloid for a single patient are likely influenced by cost and invasiveness, statistically including both will improve predictive accuracy.

We found that the nonlinear interaction between amyloid-β-PET and hippocampal volume significantly increases our model fit on unseen data, suggesting an element of synergy between the two biomarkers. By inspecting the model's decision boundaries (Figure 3), we can infer that this increased model fit is attributable to higher conversion probability values for regions with low hippocampal volume and high amyloid-β-PET values when compared to probability values obtained from a model where the biomarkers are treated independently. Our finding concurs with the results from Bilgel and colleagues (2018), where an interaction was found between hippocampal volume and amyloid-β-PET in predicting cognitive decline, in their study of n = 171 older adults from the Baltimore Longitudinal Study of Aging. Additionally, we found evidence that a three-way interaction between amyloid-β-PET, hippocampal volume and P-tau further improves model fit compared to a main-effects model, suggesting some three-way synergy between these biomarkers. We also found evidence of nonlinear interactions between hippocampal volume and: CSF P-tau, amyloid-β-PET, amyloid-β42-CSF. This supports the idea that there is a 'threshold effect' on hippocampal volume, whereby larger hippocampal volumes are associated with stable MCI, irrespective of changes in other biomarkers, while with smaller hippocampal volumes, the readouts of other biomarkers are more predictive of progressive MCI. Potentially, the presence of intact hippocampal networks enables functional compensation to ameliorate the deleterious nature of amyloid and tau deposition, however, once hippocampal atrophy crosses a certain threshold, the consequences of abnormal protein deposition become clinically manifest.

Due to the nonparametric nature of Gaussian Processes, prediction probabilities in biomarker 'space' can be used to draw conclusions about the patterns of data distributions. When examining the decision boundaries for Model 1, we observed high statistical 'certainty' in classifying participants as stable MCI in the case of high amyloid-β-CSF values, more specifically values above 192pg/mL.

Interestingly, this corresponds to the threshold proposed by Shaw and colleagues (2009), who also used ADNI. Models including high amyloid-β-CSF achieved high levels of specificity, with the individual amyloid-β-CSF model having a specificity of 0.895. This means that amyloid-β-CSF is useful for indicating that an individual is stable MCI, but given the sensitivity of 0.625, is less valuable in identifying cases of progressive MCI.

In terms of placing our Gaussian Process approach to MCI conversion prediction in literature in terms of prediction accuracy, we have extracted the following papers from a recent review (Rathore *et al.*, 2017). Cheng and colleagues (Cheng *et al.*, 2015) used a Multimodal manifold-regularized transfer learning with semi-supervised learning on MRI, PET scans and CSF features to arrive at an AUC of 0.852 (Accuracy=80.1%; Sensitivity = 85.3%; Specificity = 73.3%). Korolev and colleagues (2016) used the probabilistic multiple kernel learning classifier, obtaining AUC = 0.87 (Accuracy = 80%; Sensitivity = 83%; Specificity = 76%). Moradi and colleagues (Moradi *et al.*, 2015) achieved an AUC of 0.90 (Accuracy=82%; Specificity=74%; Sensitivity=87%) using a univariate structural MRI biomarker alongside a variety of cognitive scores. Besides these, Hor and colleagues(2016) implemented a Scandent tree approach on T1-weighted MRI ROI and global measures stemming from both FDG-PET and AV45-PET scans (Accuracy = 0.815; Sensitivity = 0.831; Specificity = 0.803; AUC = 0.872). In our work, the three-way interaction model 3 obtained a mean AUC of 0.865 (Accuracy=77.8%; Sensitivity=72.5%; Specificity=83.2%), which is comparable in accuracy to those achieved in the aforementioned papers even in light of the low number of biomarkers used and their global nature.

Our study has some important strengths and weaknesses. Ours is the first study to model nonlinear interactions between biomarkers in predicting MCI conversion to Alzheimer's, properly utilising the available information in a more biologically-valid manor. Here, we focused on model prediction, unlike previous work on interactions in MCI conversion (Fortea *et al.*, 2014; Pascoal *et al.*, 2017b), that relied on making inferences based solely on p-values. Recently, Bzdok and colleagues (2018a) highlighted the diverging end results between classical statistics and machine learning, with the former drawing population level inferences from samples, whereas the latter is seeking to find generalisable predictive patterns. In further work, Bzdok and colleagues (Bzdok *et al.*, 2018b) showed that low p-values do not necessarily translate to generalisable biomarkers in out-of-sample data. Our model offers a robust and interpretable framework by which we can visualize how biomarkers dynamically interact and how those interactions affect the decision boundaries of classifying participants as stable MCI or progressive MCI. For example, this framework could be used in designing clinical trials to assess how much change in a given biomarker must occur for an

individual to move to from being at low risk from conversion from MCI to Alzheimer's to being at high risk (i.e., moving from blue regions to red in Figure 3).

Weaknesses of the current study include the limited sample size and lack of a replication dataset. While we did use ‘held-out’ data to test model generalisability, we were unable to test the predictive performance of our models to truly independent data. This is one key limitation of multi-modality prediction models, as beyond ADNI, datasets containing MRI, amyloid-PET and CSF measures are challenging to acquire and generally not openly-available to the research community. Another limitation is that we focused on the MCI stage of the disease. Evidence suggests that Alzheimer’s pathogenesis commences years prior to any cognitive symptoms, so future work should focus on younger, at-risk groups, in order to maximise the window for interventions prior to Alzheimer’s disease manifestation. Furthermore, the diagnostic stages defined in ADNI are made clinically, while the gold standard for AD diagnosis is post-mortem. Potentially, some of the clinical assessments are inaccurate.

In conclusion, our findings suggest that multiple underlying neurobiological processes both act independently and interact in a nonlinear fashion during progression from MCI to Alzheimer’s. By capturing atrophy (hippocampal volume), amyloid-β deposition (using PET) and neurofibrillary tangle formation (CSF P-tau) in a nonlinear interactive model, can better fit models to predict conversion than independent effects alone, though main-effects multi-modality model still offer reasonable performance. The impact of modelling nonlinear interactions implies that threshold effects and pathological ‘plateaus’ are present during disease progression and that measuring multiple biomarkers will be necessary to best predict outcomes. The current data do not suggest clinically meaningful benefits of nonlinear-interaction models yet, though our novel visualisation method could be helpful in certain clinical contexts and provides strong face validity for our approach. Finally, multi-faceted therapeutic interventions are likely to be necessary, as simply influencing the levels of a single biomarker will be insufficient to modify the disease in all individuals.

Acknowledgements

Data collection and sharing for this project was funded by the Alzheimer's Disease Neuroimaging Initiative (ADNI) (National Institutes of Health Grant U01 AG024904) and DOD ADNI (Department of Defense award number W81XWH-12-2-0012). ADNI is funded by the National Institute on Aging, the National Institute of Biomedical Imaging and Bioengineering, and through generous contributions from the following: AbbVie, Alzheimer's Association; Alzheimer's Drug Discovery Foundation; Araclon Biotech; BioClinica, Inc.; Biogen; Bristol-Myers Squibb Company; CereSpir, Inc.; Cogstate; Eisai Inc.; Elan Pharmaceuticals, Inc.; Eli Lilly and Company; EuroImmun; F. Hoffmann-La Roche Ltd and its affiliated company Genentech, Inc.; Fujirebio; GE Healthcare; IXICO Ltd.; Janssen Alzheimer Immunotherapy Research & Development, LLC.; Johnson & Johnson Pharmaceutical Research & Development LLC.; Lumosity; Lundbeck; Merck & Co., Inc.; Meso Scale Diagnostics, LLC.; NeuroRx Research; Neurotrack Technologies; Novartis Pharmaceuticals Corporation; Pfizer Inc.; Piramal Imaging; Servier; Takeda Pharmaceutical Company; and Transition Therapeutics. The Canadian Institutes of Health Research is providing funds to support ADNI clinical sites in Canada. Private sector contributions are facilitated by the Foundation for the National Institutes of Health (www.fnih.org). The grantee organization is the Northern California Institute for Research and Education, and the study is coordinated by the Alzheimer's Therapeutic Research Institute at the University of Southern California. ADNI data are disseminated by the Laboratory for Neuro Imaging at the University of Southern California.

Funding

Sebastian Popescu is funded by an EPSRC Centre for Doctoral Training studentship award to Imperial College London. James Cole is funded by a UKRI Innovation Fellowship. PMM acknowledges generous personal and research support from the Edmond J Safra Foundation and Lily Safra, an NIHR Senior Investigator Award and the UK Dementia Research Institute.

Competing interests

James Cole is a scientific advisor to and shareholder in Brain Key, a medical image analysis software company. PMM acknowledges consultancy fees from Roche, Adelphi Communications, Celgene and Biogen. He has received honoraria or speakers' honoraria from Novartis, Biogen and Roche and has received research or educational funds from Biogen, Novartis, GlaxoSmithKline and Nodthera. He is a member of the Scientific Advisory Board to the Board of Ipsen Pharmaceuticals.

References

Aizenstein HJ, Nebes RD, Saxton JA, Price JC, Mathis CA, Tsopelas ND, *et al*. Frequent amyloid deposition without significant cognitive impairment among the elderly. Archives of neurology 2008; 65(11): 1509-17.

Ashburner J. A fast diffeomorphic image registration algorithm. Neuroimage 2007; 38(1): 95-113.

Bilgel M, An Y, Helphrey J, Elkins W, Gomez G, Wong DF, *et al.* Effects of amyloid pathology and neurodegeneration on cognitive change in cognitively normal adults. Brain 2018; 141(8): 2475-85.

Brookmeyer R, Johnson E, Ziegler-Graham K, Arrighi HM. Forecasting the global burden of Alzheimer's disease. Alzheimer's & dementia 2007; 3(3): 186-91.

Bzdok D, Altman N, Krzywinski M. Points of significance: statistics versus machine learning. Nature Methods 2018a: 1-7.

Bzdok D, Engemann D-A, Grisel O, Varoquaux G, Thirion B. Prediction and inference diverge in biomedicine: Simulations and real-world data. bioRxiv 2018b: 327437.

Caminiti SP, Ballarini T, Sala A, Cerami C, Presotto L, Santangelo R, *et al.* FDG-PET and CSF biomarker accuracy in prediction of conversion to different dementias in a large multicentre MCI cohort. NeuroImage: Clinical 2018; 18: 167-77.

Caroli A, Prestia A, Galluzzi S, Ferrari C, Van Der Flier WM, Ossenkoppele R, *et al.* Mild cognitive impairment with suspected nonamyloid pathology (SNAP) Prediction of progression. Neurology 2015; 84(5): 508-15.

Chaudhuri A. Multiple sclerosis is primarily a neurodegenerative disease. Journal of neural transmission 2013; 120(10): 1463-6.

Cheng B, Liu M, Suk H-I, Shen D, Zhang D, Initiative AsDN, *et al.* Multimodal manifold-regularized transfer learning for MCI conversion prediction. Brain imaging and behavior 2015; 9(4): 913-26.

Chevan A, Sutherland M. Hierarchical Partitioning. The American Statistician 1991; 45(2): 90-6.

Cole JH. Neuroimaging Studies Illustrate the Commonalities Between Ageing and Brain Diseases. BioEssays 2018; 40(7): 1700221.

Cole JH, Annus T, Wilson LR, Remtulla R, Hong YT, Fryer TD, *et al.* Brain-predicted age in Down Syndrome is associated with β-amyloid deposition and cognitive decline. Neurobiology of aging 2017a; 56: 41-9.

Cole JH, Leech R, Sharp DJ, for the Alzheimer's Disease Neuroimaging Initiative. Prediction of brain age suggests accelerated atrophy after traumatic brain injury. Ann Neurol 2015; 77(4): 571-81.

Cole JH, Poudel RPK, Tsagkrasoulis D, Caan MWA, Steves C, Spector TD, *et al.* Predicting brain age with deep learning from raw imaging data results in a reliable and heritable biomarker. NeuroImage 2017b; 163C: 115-24.

Cole JH, Ritchie SJ, Bastin ME, Valdes Hernandez MC, Munoz Maniega S, Royle N, *et al.* Brain age predicts mortality. Molecular psychiatry 2018; 23: 1385-92.

Cole JH, Underwood J, Caan MWA, De Francesco D, van Zoest RA, Leech R, *et al.* Increased brain-predicted aging in treated HIV disease. Neurology 2017c; 88(14): 1349-57.

Draganski B, Lutti A, Kherif F. Impact of brain aging and neurodegeneration on cognition: evidence from MRI. Curr Opin Neurol 2013; 26(6): 640-5.

Dubois B, Feldman HH, Jacova C, Hampel H, Molinuevo JL, Blennow K, *et al.* Advancing research diagnostic criteria for Alzheimer's disease: the IWG-2 criteria. The Lancet Neurology 2014; 13(6): 614-29.

Duvenaud DK, Nickisch H, Rasmussen CE. Additive gaussian processes. Advances in neural information processing systems; 2011 2011//; 2011. p. 226-34.

Fjell AM, Walhovd KB, Fennema-Notestine C, McEvoy LK, Hagler DJ, Holland D, *et al.* One-year brain atrophy evident in healthy aging. Journal of Neuroscience 2009; 29(48): 15223-31.

Fortea J, Vilaplana E, Alcolea D, Carmona-Iragui M, Sánchez-Saudinos M-B, Sala I, *et al.* Cerebrospinal fluid β-amyloid and phospho-tau biomarker interactions affecting brain structure in preclinical Alzheimer disease. Ann Neurol 2014; 76(2): 223-30.

Franke K, Gaser C. Longitudinal Changes in Individual BrainAGE in Healthy Aging, Mild Cognitive Impairment, and Alzheimer's Disease. GeroPsych 2012.

Franke K, Ziegler G, Klöppel S, Gaser C, for the Alzheimer's Disease Neuroimaging Initiative. Estimating the age of healthy subjects from T1-weighted MRI scans using kernel methods: exploring the influence of various parameters. Neuroimage 2010; 50(3): 883-92.

Gaser C, Franke K, Klöppel S, Koutsouleris N, Sauer H, for the Alzheimer's Disease Neuroimaging Initiative. BrainAGE in mild cognitive impaired patients: predicting the conversion to Alzheimer's disease. PloS one 2013; 8(6): e67346.

Hensman J, Matthews AGdG, Ghahramani Z. Scalable variational Gaussian process classification. 2015.

Hor S, Moradi M. Learning in data-limited multimodal scenarios: Scandent decision forests and tree-based features. Medical image analysis 2016; 34: 30-41.

Jack CR, Petersen RC, Xu YC, O'Brien PC, Smith GE, Ivnik RJ, *et al.* Prediction of AD with MRI-based hippocampal volume in mild cognitive impairment. Neurology 1999; 52(7): 1397-.

Jack Jr CR, Knopman DS, Jagust WJ, Petersen RC, Weiner MW, Aisen PS, *et al.* Update on hypothetical model of Alzheimer's disease biomarkers. Lancet neurology 2013; 12(2): 207.

Jack Jr CR, Knopman DS, Jagust WJ, Shaw LM, Aisen PS, Weiner MW, *et al.* Hypothetical model of dynamic biomarkers of the Alzheimer's pathological cascade. The Lancet Neurology 2010; 9(1): 119-28.

Jack Jr CR, Therneau TM, Wiste HJ, Weigand SD, Knopman DS, Lowe VJ, *et al.* Transition rates between amyloid and neurodegeneration biomarker states and to dementia: a population-based, longitudinal cohort study. The Lancet Neurology 2016; 15(1): 56-64.

Jagust WJ, Landau SM, Koeppe RA, Reiman EM, Chen K, Mathis CA, *et al.* The Alzheimer's Disease Neuroimaging Initiative 2 PET Core: 2015. Alzheimer's & Dementia: The Journal of the Alzheimer's Association 2015; 11(7): 757-71.

Korolev IO, Symonds LL, Bozoki AC, Initiative AsDN, others. Predicting progression from mild cognitive impairment to Alzheimer's dementia using clinical, MRI, and plasma biomarkers via probabilistic pattern classification. PloS one 2016; 11(2): e0138866.

Laakso MP, Partanen K, Riekkinen P, Lehtovirta M, Helkala EL, Hallikainen M, *et al.* Hippocampal volumes in Alzheimer's disease, Parkinson's disease with and without dementia, and in vascular dementia An MRI study. Neurology 1996; 46(3): 678-81.

Li H, Liu Y, Gong P, Zhang C, Ye J, Initiative ADN, *et al.* Hierarchical interactions model for predicting Mild Cognitive Impairment (MCI) to Alzheimer's Disease (AD) conversion. PloS one 2014; 9(1): e82450.

Lorenzetti V, Allen NB, Fornito A, Yücel M. Structural brain abnormalities in major depressive disorder: a selective review of recent MRI studies. Journal of affective disorders 2009; 117(1-2): 1-17.

Mattsson N, Insel PS, Donohue M, Landau S, Jagust WJ, Shaw LM, *et al.* Independent information from cerebrospinal fluid amyloid-β and florbetapir imaging in Alzheimer's disease. Brain 2014; 138(3): 772-83.

Moradi E, Pepe A, Gaser C, Huttunen H, Tohka J, Initiative AsDN, *et al.* Machine learning framework for early MRI-based Alzheimer's conversion prediction in MCI subjects. Neuroimage 2015; 104: 398-412.

Olea PP, Mateo-Tomás P, De Frutos Á. Estimating and modelling bias of the hierarchical partitioning public-domain software: implications in environmental management and conservation. PloS one 2010; 5(7): e11698.

Pardoe HR, Cole JH, Blackmon K, Thesen T, Kuzniecky R, Investigators HEP, *et al.* Structural brain changes in medically refractory focal epilepsy resemble premature brain aging. Epilepsy research 2017; 133: 28-32.

Pascoal TA, Mathotaarachchi S, Mohades S, Benedet AL, Chung C-O, Shin M, *et al.* Amyloid-β and hyperphosphorylated tau synergy drives metabolic decline in preclinical Alzheimer's disease. Molecular psychiatry 2017a; 22(2): 306.

Pascoal TA, Mathotaarachchi S, Shin M, Benedet AL, Mohades S, Wang S, *et al.* Synergistic interaction between amyloid and tau predicts the progression to dementia. Alzheimer's & Dementia 2017b; 13(6): 644-53.

Pellegrini E, Ballerini L, Hernandez MdCV, Chappell FM, González-Castro V, Anblagan D, *et al.* Machine learning of neuroimaging to diagnose cognitive impairment and dementia: a systematic review and comparative analysis. arXiv preprint arXiv:180401961 2018.

Rasmussen CE, Williams CKI. Gaussian Processes for Machine Learning: MIT Press; 2006.

Rathore S, Habes M, Iftikhar MA, Shacklett A, Davatzikos C. A review on neuroimaging-based classification studies and associated feature extraction methods for Alzheimer's disease and its prodromal stages. NeuroImage 2017; 155: 530-48.

Sarica A, Cerasa A, Quattrone A. Random Forest Algorithm for the Classification of Neuroimaging Data in Alzheimer's Disease: A Systematic Review. Frontiers in Aging Neuroscience 2017; 9: 329.

Schoonenboom NSM, Reesink FE, Verwey NA, Kester MI, Teunissen CE, Van De Ven PM, *et al.* Cerebrospinal fluid markers for differential dementia diagnosis in a large memory clinic cohort. Neurology 2011: WNL-0b013e31823ed0f0.

Schrouff J, Rosa MJ, Rondina JM, Marquand AF, Chu C, Ashburner J, *et al.* PRoNTo: Pattern recognition for neuroimaging toolbox. Neuroinformatics 2013; 11(3): 319-37.

Shaw LM, Vanderstichele H, Knapik-Czajka M, Clark CM, Aisen PS, Petersen RC, *et al.* Cerebrospinal fluid biomarker signature in Alzheimer's disease neuroimaging initiative subjects. Ann Neurol 2009; 65(4): 403-13.

Sperling RA, Aisen PS, Beckett LA, Bennett DA, Craft S, Fagan AM, *et al.* Toward defining the preclinical stages of Alzheimer's disease: Recommendations from the National Institute on Aging-Alzheimer's Association workgroups on diagnostic guidelines for Alzheimer's disease. Alzheimer's & dementia 2011; 7(3): 280-92.

Tatsuoka C, Tseng H, Jaeger J, Varadi F, Smith MA, Yamada T, *et al.* Modeling the heterogeneity in risk of progression to Alzheimer's disease across cognitive profiles in mild cognitive impairment. Alzheimer's research & therapy 2013; 5(2): 14.

Tziortzi AC, Searle GE, Tzimopoulou S, Salinas C, Beaver JD, Jenkinson M, *et al.* Imaging dopamine receptors in humans with [11C]-(+)-PHNO: Dissection of D3 signal and anatomy. NeuroImage 2011; 54(1): 264-77.

Villemagne VL, Pike KE, Chételat G, Ellis KA, Mulligan RS, Bourgeat P, *et al.* Longitudinal assessment of Aβ and cognition in aging and Alzheimer disease. Ann Neurol 2011; 69(1): 181-92.

Xu W-L, Caracciolo B, Wang H-X, Santoni G, Winblad B, Fratiglioni L. Accelerated progression from mild cognitive impairment to dementia among APOE e4\e4 carriers. Journal of Alzheimer's Disease 2013; 33(2): 507-15.